

ON THE MULTIFRAGMENTATION AND PHASE TRANSITION IN THE PERSPECTIVES OF DIFFERENT n -BODY DYNAMICAL MODELS*

ROHIT KUMAR^a, SAMIKSHA SOOD^a, ARUN SHARMA^b, RAJEEV K. PURI^a

^aDepartment of Physics, Panjab University, Chandigarh, 160014, India

^bG.D. College, Thanna Mandi, Rajouri, Jammu and Kashmir, 185212, India

(Received December 13, 2017)

We study central reactions of $^{40}\text{Ar}+^{45}\text{Sc}$ in the energy range of 15–115 MeV/nucleon using two different n -body dynamical models. In particular, we use the Quantum Molecular Dynamics model and its modified isospin-dependent version. The charge distribution of emitted intermediate mass fragments [$3 \leq Z_f \leq 12$] is fitted using the power law function [$Y(Z_f) = Y_0 Z_f^{-\tau}$]. We discuss the differences in the results obtained using the two models for the critical point of the liquid–gas phase transition in nuclear matter.

DOI:10.5506/APhysPolB.49.301

1. Introduction

Based on the similarity between the nucleon–nucleon interactions in nuclear matter and van der Waals' real gases, the multifragmentation phenomenon [1, 2] is often linked to the liquid–gas phase transition. Curtin, Toki and Scott were among the first to point out that if fragment formation in a heavy-ion collision occurs at the critical point of the liquid–gas phase transition, the fragments must show some characteristic signal [3]. They also shown that such a signal can be obtained from the fragment charge (mass) spectra, if fitted according to the power law expression of the form $Y(Z_f) = Y_0 Z_f^{-\tau}$ [$Y(A_f) = Y_0 A_f^{-\tau}$]. At the critical point, τ showed a minimum, a behavior that was in accordance with the earlier predictions of the Fisher droplet model.

* Presented at the XXXV Mazurian Lakes Conference on Physics, Piaski, Poland, September 3–9, 2017.

Earlier experiments on multifragmentation were based on inclusive charge distributions of fragments produced in proton-induced reactions. Therefore, contradictory results were observed in many experiments and the interpretation of the liquid–gas phase transition in nuclear matter was disputed [4, 5]. Following later exclusive studies, the link between multifragmentation and the liquid–gas phase transition has been well-established both on the experimental as well as the theoretical front [6, 7]. For example, Li *et al.* [6] fitted with the power law the fragment-charge distribution obtained in the central reactions of $^{40}\text{Ar}+^{45}\text{Sc}$ in the incident energy range of 15–115 MeV/nucleon and reported a minimum at 23.9 ± 0.7 MeV/nucleon. It is worth mentioning here that in the studies performed with highly charged reaction partners, no minima in τ were observed [8]. The Coulomb force was reported to be the main culprit for this behavior.

In the recent years, the nuclear community has become much interested in understanding differences between various transport models (based on one-body as well as on n -body theories) that are used to study heavy-ion collisions at intermediate energies. The results obtained using different transport models for particle production, rapidity distribution, transverse spectra, flow, *etc.* were compared [9, 10]. Very recently, Xu *et al.* [11] reported first results of the code-comparison-collaboration, where comparison between the technical aspects of various transport models was made using non-observable quantities and keeping almost the same initial conditions. Their study reflects a strong need to understand the structure of and the differences between transport models, in order to understand the dynamics of heavy-ion collisions in a model-independent way. In the present study, we will discuss the results of two of the widely used n -body transport models named Quantum Molecular Dynamics (QMD) model and Isospin-dependent Quantum Molecular Dynamics (IQMD) model [12, 13] on the critical point in the liquid–gas phase transition in nuclear matter.

2. The models

2.1. Quantum Molecular Dynamics model

The Quantum Molecular Dynamics (QMD) model [12, 14–16] is an n -body transport model that simulates the heavy-ion collisions on an event-by-event basis. In the first step, the nuclei are initialized in coordinate and momentum space. The position of each nucleon is assigned randomly inside a sphere with radius $R = 1.14 A^{1/3}$ and momentum values between 0 and P_F (where P_F is the local Fermi momentum, $P_F = \sqrt{-2mU(r_i)}$, with $U(r_i)$ being the local potential of nucleons) using the Monte Carlo method. Here, each nucleon is represented by a Gaussian wave packet with a constant width and the total wave function of the n -body system is constructed by multiplying the one-body wave functions of nucleons.

In the second step, the successfully initialized nuclei are boosted towards each other with a proper center-of-mass energy. The propagation of each nucleon in the phase space is described using Hamilton's classical equations of motion

$$\dot{\vec{r}}_i = \frac{\partial H}{\partial \vec{p}_i}; \quad \dot{\vec{p}}_i = -\frac{\partial H}{\partial \vec{r}_i}, \quad (1)$$

where the Hamiltonian H is expressed as

$$H = \sum_i \frac{p_i^2}{2m_i} + V^{\text{Tot}}, \quad (2)$$

with V^{Tot} comprising Skyrme, Yukawa and Coulomb potentials.

In the last step, if two nucleons approach closer than $\sqrt{\frac{\sigma^{\text{free}}}{\pi}}$, they are scattered stochastically with the nucleon–nucleon (nn) scattering cross section parameterized as proposed by Cugnon *et al.* [12].

2.2. Isospin-dependent Quantum Molecular Dynamics model

The Isospin-dependent Quantum Molecular Dynamics (IQMD) [13] model is an extension of the QMD model, the former being based on the Vlasov–Uehling–Uhlenbeck (VUU) code, whereas the latter is based on the Boltzmann–Uehling–Uhlenbeck (BUU) code. In the IQMD model, different charge states of nucleons, deltas and pions are treated explicitly. Moreover, the isospin degree of freedom (which is not included in the QMD model) has been incorporated in the model in the nn scattering cross section, the Coulomb potential as well as the symmetry potential.

The IQMD model, like the QMD model, is also a three step model, but with certain differences in the structure of the steps. For instance, during the initialization, the IQMD model assigns coordinates within a sphere of radius $R = 1.12 A^{1/3}$ and momentum values are assigned between 0 and P_F . Here, P_F (global Fermi momentum) is calculated using the Fermi-gas model. This choice of Fermi momentum in the IQMD model makes density profiles of nuclei much smoother than in the case of the QMD model, but at the cost of binding energy, and also making the IQMD-generated nuclei more prone towards nucleon evaporation from the surface. In the IQMD model, the width of the Gaussian wave packet is dependent on the system size as compared to a constant value in the QMD model. Lastly, nn cross section is parameterized as proposed by VerWest and Arndt.

3. Results and discussion

In the present work, we simulated thousands of central events of $^{40}\text{Ar} + ^{45}\text{Sc}$ in the energy range of 15–115 MeV/nucleon. The reactions are

followed till 300 fm/c, where the interactions between the nucleons are considered to be ceased. The phase space generated using the transport models (IQMD/QMD) is subjected to the Minimum Spanning Tree (MST) method [12, 16, 17] that sorts out the fragments based on the spatial accumulation of nucleons in the coordinate space.

Figure 1 shows the fragment charge spectra for the central reactions of $^{40}\text{Ar}+^{45}\text{Sc}$ at different incident energies in the range of 15–115 MeV/nucleon. The results obtained using QMD (IQMD) model are represented by triangles (circles). From the figure, one can see the steepening of the fragment charge distribution with incident energy (except for the QMD model calculations at 15 and 20 MeV/nucleon). This can be understood on the basis of the energy deposited into the composite system formed during the early stages of a heavy-ion reaction. The greater energy is deposited, the more probable is the breaking of the system, making it less likely to obtain larger charge fragments

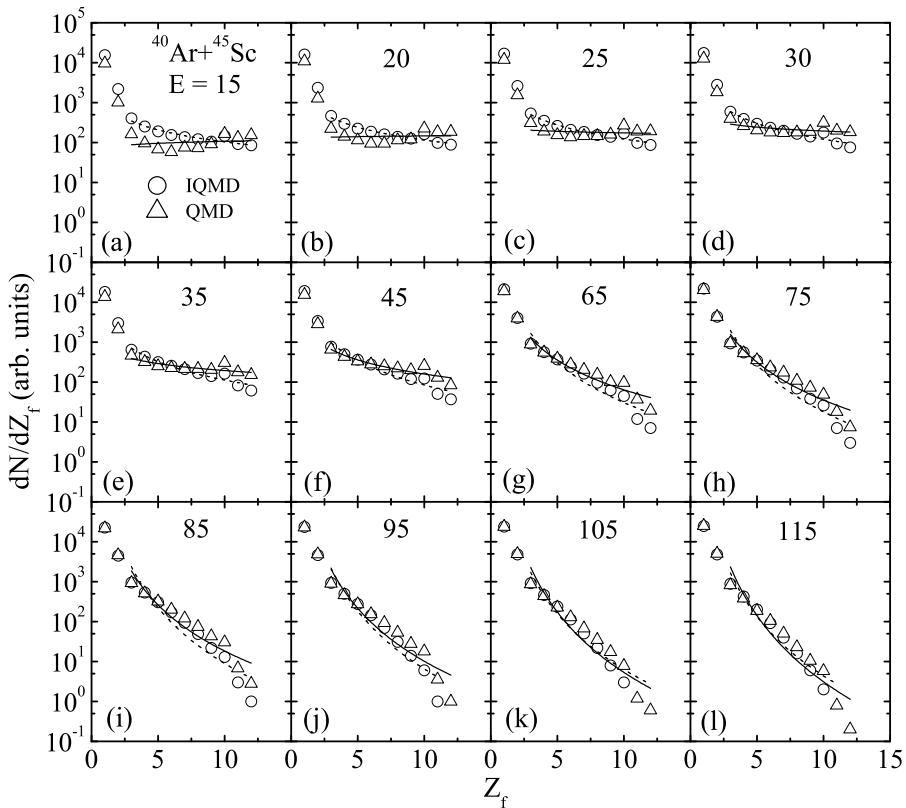


Fig. 1. Fragment charge spectra ($Z_f > 12$ not shown for clarity) of the central reactions of $^{40}\text{Ar}+^{45}\text{Sc}$ at different beam energies in the range of 15–115 MeV/nucleon. Triangles (circles) represent the calculations using QMD (IQMD) model. Projectile incident energy E is in MeV/nucleon.

compared to lighter charge fragments. These results are consistent with the earlier results reported in Refs. [6, 8]. From the figure, one can clearly see that at lower incident energies (below 65 MeV/nucleon), the results of IQMD and QMD models differ significantly. We see more small fragments and fewer larger fragments with the IQMD model as compared to the QMD model. This is due to a higher value of the Fermi momentum in the IQMD model that causes more breaking in the system even at lower incident energies, whereas at higher incident energies, this effect becomes less pronounced and we see almost the same fragment charge spectra for both models.

The fragment charge spectra at different incident energies displayed in Fig. 1 are fitted with the power law of the form of $Y(Z_f) = Y_0 Z_f^{-\tau}$. We have fitted only intermediate mass fragments (IMF, $3 \leq Z_f \leq 12$). The lines are to guide the eye. The critical parameter τ , obtained from the power law fitting, is plotted against incident energy in Fig. 2. From the figure, we see significantly different results for τ at lower incident energies for the two models. We also notice that a minimum is observed with the QMD model at 18 MeV/nucleon. On the other hand, the IQMD model shows a flat behavior. It was investigated by Sharma *et al.* [18, 19], and the Coulomb interaction was suggested to be the main culprit, consistent with the results of Ref. [8]. We also note that the higher value of the Fermi momentum makes the τ minimum vanish by shifting it to lower incident energies (beyond the limit of the IQMD model). The fact that no critical point was observed with the IQMD model, whereas our QMD calculations showed a critical point, suggests that the internal structure of the models can lead to different results. Therefore, a deeper understanding of the internal structures of transport models is needed to better understand the dynamics of heavy-ion reactions.

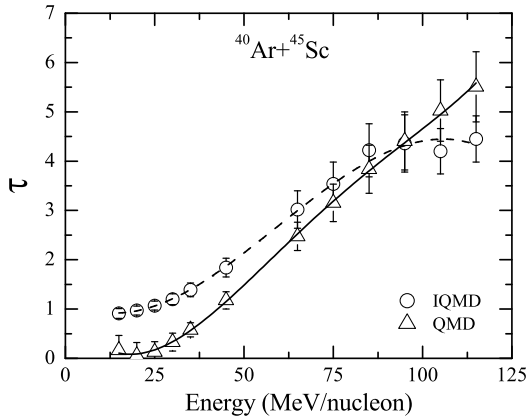


Fig. 2. Extracted values of the critical parameter τ from the power law fit of intermediate mass fragments. The symbols have the same meaning as in Fig. 1.

4. Summary

We studied central reactions of $^{40}\text{Ar}+^{45}\text{Sc}$ in the energy range of 15–115 MeV/nucleon using two different n -body dynamical models, *i.e.* QMD and IQMD models. The charge distribution of the emitted IMFs [$3 \leq Z_f \leq 12$] is fitted using the power law and the critical point is explored in the light of the two models. We observed that the change in the primary model leads to different results on the critical point of the liquid–gas phase transition.

REFERENCES

- [1] G.F. Peaslee *et al.*, *Phys. Rev. C* **49**, 2271(R) (1994).
- [2] B. Borderie *et al.*, *Prog. Part. Nucl. Phys.* **61**, 551 (2008).
- [3] M.W. Curtin, H. Toki, D.K. Scott, *Phys. Lett. B* **123**, 289 (1983).
- [4] G. Peilert *et al.*, *Phys. Rev. C* **39**, 1402 (1989).
- [5] N.T. Porile *et al.*, *Phys. Rev. C* **39**, 1914 (1989).
- [6] T. Li *et al.*, *Phys. Rev. C* **49**, 1630 (1994).
- [7] Y.G. Ma, W.Q. Shen, *Phys. Rev. C* **51**, 710 (1995).
- [8] M.D. Agostino *et al.*, *Phys. Rev. Lett.* **75**, 4373 (1995); C. Williams *et al.*, *Phys. Rev. C* **55**, 2132(R) (1997).
- [9] E.E. Kolomeitsev *et al.*, *J. Phys. G: Nucl. Part. Phys.* **31**, S741 (2005).
- [10] Workshop web site: <http://www.pgysics.sjtu.edu.cn/hic2014/>
- [11] J. Xu *et al.*, *Phys. Rev. C* **93**, 044609 (2016).
- [12] J. Aichelin, *Phys. Rep.* **202**, 233 (1991).
- [13] C. Hartnack *et al.*, *Eur. Phys. J. A* **1**, 151 (1998).
- [14] R.K. Puri, S. Kumar, *Phys. Rev. C* **57**, 2744 (1998).
- [15] J. Singh *et al.*, *Phys. Rev. C* **63**, 054603 (2001); R.K. Puri *et al.*, *Phys. Rev. C* **54**, R28 (1996).
- [16] S. Kumar, R.K. Puri, *Phys. Rev. C* **58**, 2858 (1998); **58**, 320 (1998); **60**, 054607 (1999); S. Goyal, R.K. Puri, *Phys. Rev. C* **83**, 047601 (2011).
- [17] R. Kumar *et al.*, *Phys. Rev. C* **89**, 064608 (2014); *J. Phys. G: Nucl. Part. Phys.* **43**, 025104 (2016); *Eur. Phys. J. A* **52**, 112 (2016).
- [18] A. Sharma *et al.*, *Nucl. Phys. A* **945**, 95 (2016).
- [19] A. Sharma, A. Bharti, *Eur. Phys. J. A* **52**, 42 (2016).